Reaction rate and collisional efficiency of the rhodopsin-transducin system in intact retinal rods

Martina Kahlert and Klaus Peter Hofmann
Institut für Biophysik und Strahlenbiologie, Albert-Ludwigs-Universität, Albertstrasse 23, D-7800 Freiburg, Federal Republic of Germany

ABSTRACT A model of transducin activation is constructed from its partial reactions (formation of metarhodopsin II, association, and dissociation of the rhodopsin-transducin complex). The kinetic equations of the model are solved both numerically and, for small photoactivation, analytically. From data on the partial reactions in vitro, rate and activation energy profile of amplified transducin turnover are modeled and compared with measured light-scattering signals of transducin activation in intact retinal rods. The data leave one free parameter, the rate of association between transducin and rhodopsin. Best fit is achieved for an activation energy of 35 kJ/mol, indicating lateral membrane diffusion of the proteins as its main determinant. The absolute value of the association rate is discussed in terms of the success of collisions to form the catalytic complex. It is >30% for the intact retina and 10 times lower after permeabilization with *staphylococcus aureus* α-toxin. Dissociation rates for micromolar guanosinetriphosphale (GTP) (Kohl, B., and K. P. Hofmann. 1987. *Biophys. J.* 52:271–277) must be extrapolated linearly up to the millimolar range to explain the rapid transducin turnover in situ. This is interpreted by an unstable rhodopsin-transducin-GTP transient state. At the time of maximal turnover after a flash, the rate of activation is determined as 30, 120, 800, 2,500, and 4,000 activated transducins per photoactivated rhodopsin and second at 5, 10, 20, 30, 37°C, respectively.

INTRODUCTION

G-proteins function as universal transducers between extracellular signals (such as light or hormones) and intracellular second messengers (as cyclic nucleotides; reviewed by Gilman, 1987). Signal transduction starts with the transformation of the receptor protein into an activated state and formation of a complex between the receptor and the G hetrotrimeric $\alpha\beta\tau$ holoprotein. The interaction with the receptor causes an opening of the nucleotide binding site of the Gα subunit of and a replacement of initially bound GDP (inactive ligand) by the activating ligand, GTP. This exchange reaction induces the release of G_α; interaction of the activated G_α with an effector protein constitutes the subsequent step of the signal transduction pathway (for reviews, see Stryer, 1986; Liebman et al., 1987; and Chabre and Deterre, 1989).

In this study, we have explored the dynamics of the activation reaction of the rod G-protein (transducin, G_t[1]). In intact rod cells, one single molecule of the light-activated receptor rhodopsin (R*) can turn over >3,000 copies of G_t (Dawis et al., 1988). The well-known fast lateral and rotational diffusion of rhodopsin, and presumably of G_t, in the disc membrane affords sufficiently frequent collisions for a high speed of activation (Cone, 1972; Poo and Cone, 1974; Liebman and Entine, 1974). For the mean activation time in situ of one G_t molecule, the current estimation is ~1 ms per G_t (Vuong et al., 1984; Pepperberg et al., 1988). This explosive light-induced activity is in sharp contrast to the very low activity of the system in the dark, as estimated from receptor dark noise (Lamb, 1987).

The ability of the rod cell to detect single quanta (Baylor et al., 1979) critically depends on the perfection of the G activation step of signal transduction, on its fidelity, and speed. Liebman and associates have put forward the notion of a high collisional efficiency of the rhodopsin transducin system (Liebman et al., 1987), based on its membrane organization. There is still no solid molecular basis for understanding this efficiency. Some mechanistic details are emerging which might contribute to it, such as the simultaneous interaction of the proteins via several sites, involving three cytoplasmic loops of rhodopsin (Hamm et al., 1988; König et al., 1989), and preceded by a state of interaction in which the opening of the nucleotide site is induced (Kahlert et al., 1990). However, the kinetic parameters of R-G_t complex formation are sufficiently well known from measurements in vitro, including formation of the active rhodopsin intermediate, membrane diffusion, and dissociation rate (for reviews see Liebman et al., 1987;

Address correspondence to K. P. Hofmann, Institut für Biophysik und Strahlenbiologie, Albert-Ludwigs-Universität, Albertstrasse 23, D-7800 Freiburg, Federal Republic of Germany.

[1]*Abbreviations used in this paper:* AT(R)-signal, amplified transient (retina) signal; G*, activated transducin; G_t, G, G-protein of the rod, transducin; (K)LS, (kinetic) light scattering; R, rhodopsin; R*, photoactivated rhodopsin.

Hofmann, 1986). We have constructed a model of G_t activation from these data and compared it to the dynamics of the rapid G_t turnover in vivo.

The experimental assay that has enabled such a comparison comes from recent progress in measuring kinetic light scattering (KLS) in situ. Kühn et al. (1981) have disclosed the small LS changes ("signals") of rod outer segment membranes, which are evoked by flashes of visible light (Hofmann et al., 1976), as a stoichiometric measure of the binding and activation of G_t. Later work has carried this probe into structurally intact rod outer segments. By contrast to the kinetic complexity of the LS signals from isolated membranes (dominated by membrane aggregation (Lewis et al., 1984; Caretta and Stein, 1985) and/or free diffusion of G_t (Schleicher and Hofmann, 1987), signals from the native system are surprisingly simple. In all preparations which preserve the intact stack structure of the rod outer segments basically the same fast, transient increase of near infrared light scattering can be evoked by small flashes of light. Systems investigated include isolated frog ("release signal"; Vuong et al., 1984) and bovine rod outer segments ("amplified transient [AT] signal" "amplified P-signal", Kamps et al., 1985; Wagner et al., 1987) and the intact bovine retina ("ATR signal", Pepperberg et al., 1988; Kahlert and Hofmann, 1988). The question whether the signal reflected directly the free, activated G_t (Vuong et al., 1984) or its interaction with the effector phosphodiesterase (Kamps et al., 1985) has now been settled by recent observations of Bruckert et al. (1988) on electroporated (but structurally intact) rod outer segments which allow the exchange of G_t. The authors demonstrated linearity of the LS change with the amount of membrane-bound transducin, establishing their observation (the "release signal") as a stoichiometric monitor of the activated form of transducin (Bruckert et al., 1988). By the analogy of the systems, we assume the same interpretation for the ATR signal. *We note that LS changes measured in situ cannot provide a measure in absolute numbers and need an assumption in terms of the total activatable G_t pool.*

It will be seen that the available data restrict the fit between the model and the LS results to one free parameter, the rate of association between R and G_t.

For an appropriate choice of this parameter, the model fits the kinetics of G_t activation within the experimentally accessible range of temperature for intact, functioning rods as well as for an α-toxin permeabilized retina preparation which preserves the protein inventory. The interesting difference is that, in the intact rods, the collisional efficiency of R-G interaction is close to 100%, while it is lower by one order of magnitude in the permeabilized rods.

MATERIALS AND METHODS

Preparation

Bovine retinae were prepared as described by Pepperberg et al. (1988) and Kahlert (1986): bovine eyes from a local abbatoir were stored in the dark and dissected under dim red light within ~1 h after the animal's death. Circular pieces of retina (7 mm diam) were isolated from the eyecup and fixed on a nylon net within a holder in a transparent chamber (volume 1 ml). The chamber was continuously superfused with oxygenated Ringer's solution. The rods in this preparation were intact as regards their metabolic and signal transducing abilities (Pepperberg et al., 1988).

Permeabilization of the retinae was performed as described by Kahlert and Hofmann (1988): 1 mg α-toxin of *staphylococcus aureus* (gift from Behring Werke, Marburg, FRG) in 100 μl isotonic Ringer's solution was dropped on the receptor side of the retina and incubated for 5 min. The holder was placed in the chamber filled with Ringer's solution.

Solutions

Intact retina: Cholin chloride 134 mM, KCl 2 mM, $CaCl_2$ 0.1 mM, $MgCl_2$ 0.1 mM, NaH_2PO_4 1.5 mM, Na_2HPO_4 4.2 mM, glucose 5 mM, L-aspartate 2 mM, adjusted to pH 7.2 with NaOH.

Permeabilized retina: KCl 120 mM, NaCl 1.5 mM, $MgCl_2$ 5 mM, Hepes 20 mM; GTP 1 mM; in some experiments, 5 mM glucose was added, with no effect on the results; this solution was adjusted to pH 7.6 with KOH.

All chemicals were of the highest purity available.

Measuring technique

The measuring technique was basically the same as described by Kahlert (1986) and Pepperberg et al. (1988). The incident beam (840 nm) was provided by an LED (Hitachi HLP 60R; Hitachi America, San Jose, CA) and entered the retina normal to its plane on the vitreal surface (cf. Fig. 1). The scattered light was collected by a fresnel lens system and focused onto a solid-state photodetector (Centronics OSD 100 5-T). The scattering angle could be selected with different diaphragms; standard angle was 6°–10°. Scattering changes (ΔI) were normalized to the basic intensity of scattered light (I). Such a normalization eliminates apparative effects (properties of fresnel lenses, width of diaphragms) on the angular dependence of the signal amplitude.

To measure the correct angular dependence of the basic scattering intensity (I) before flash excitation, the fresnel lenses were replaced by a small detector which allows the angular range to be scanned. The measured $I(\Theta)$ was corrected with $1/\cos^3$ to account for the geometry of detection (detector moves in a plane, implying a correction of $1/\cos\Theta$ for the oblique incidence of the detecting area and $1/\cos^2\Theta$ for the varying distance between sample and detector). With this $I(\Theta)$ and the $\Delta I/I(\Theta)$ of the scattering change, the correct $\Delta I(\Theta)$ was obtained. Stimulating green flashes (20 μs; EG&G FX-133 flashgun) were delivered to the retina via a fiber optic guide at an inclination of 10° relative to the measuring beam. Flash intensity could be attenuated with neutral density filters. It will be expressed as the fractional bleach R^*/R. Calibration of rhodopsin photoactivation was carried out by spectrophotometry of intact retinae.

The amplified photodetector output was fed into a Nicolet 2090IIIA recorder (Nicolet Deutschland gmbH, Offenbach, FRG) connected to a computer. The temperature was measured by a sensor within the chamber.

Scattering characteristics of the retina

Fig. 1 *C* compares the angular dependence of the basic scattering (I) and $I + \Delta I$ of a bovine retina. The flash induced scattering change $\Delta I(\Theta)$ is derived from $I(\Theta)$ and $\Delta I/I(\Theta)$ at the peak of the ATR signal as described above; for better comparison, ΔI is scaled up by a factor of 200.

The measured baseline scattering curve of the bovine retina is well described by a Gaussian function with $\sigma \approx 10°$ sitting on a $\cos^2$ curve. Laser diffraction of an electron micrograph from this layer (courtesy of M. Drechsler, not shown) yields experimentally a zero-order maximum similar to the experimental Gaussian curve from the retina, indicating that this characteristic arises predominantly from the quasi-crystalline order of the retinal receptor layer.

The flash-induced scattering change (ΔI) reproduces only the Gaussian component, in agreement with the generation of the signal in the rod outer segments, not involving postponed neuronal activities (Pepperberg et al., 1988).

The fact that ΔI simply scales up the Gaussian component of I implies that the scattering change ΔI is proportional to the basic scattering intensity of the signal generating structure. This is consistent with the assumption that the signal is caused by a homogeneous change of polarizability within the ROS arising from the activated transducin molecules.

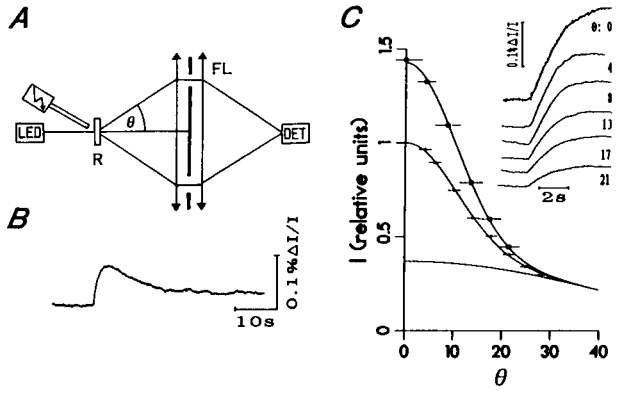

FIGURE 1 Setup and example for measuring near infrared light scattering changes. (*A*) LED, light emitting diode (880 nm); R, chamber containing isolated retina; FL, fresnel lens system with diaphragm; DET, silicon photodetector; Θ, scattering angle. (*B*) Measuring example, ATR ("*a*mplified *t*ransient in the *r*etina") signal from an α-toxin permeabilized bovine retina. See text for further details. (*C*) Relationship between the basic scattering of the retina (I) and the flash induced scattering change (ΔI, ATR signal). (*Inset*) ATR signals from an α-toxin permeabilized retina (GTP 1 mM, $R^*/R = 2.7 \cdot 10^{-4}$); numbers indicate the scattering angle Θ where the signals were recorded. (*Small symbols*) Angular dependence of the basic scattering of the same retina (*relative units*); a fit to the data by $I = a \cdot \exp(-\Theta^2/2\sigma^2) + b \cdot \cos^2\Theta$ (*solid line*) yields $\sigma = 10$; a separate solid line shows the term $b \cdot \cos^2\Theta$. (*Large symbols*) Angular dependence of $I + \Delta I$; ΔI is derived from the signals in the inset and upscaled by a factor of 200; $I + \Delta I$ is fitted by the same function as I, yielding the same values for b and σ. The horizontal bars denote the angular range of detection.

Measuring protocol

Both the intact and the permeabilized retina produce stable flash responses which allow measurements for several hours. In the permeabilized preparation, this requires the presence of GTP in the medium. Absence of GTP causes irreversible decline of the signal within ~1 h.

Signals were recorded at intervals that insured full recovery from the previous flash (1–4 min, dependent on temperature). Typically, two recordings were averaged. Temperature-dependent measurements typically involved a cooling down of the retina to ~5°C and subsequent warming up, and a warming up to 30°–40°C and subsequent cooling down, both starting and ending at room temperature (temperature changes 7–15°/h).

Model calculations

Numerical solutions of differential equations were obtained using the method of Euler; the time interval of iteration steps dt was 10% of the time constant of the fastest reaction, reduction of dt by a factor of 5 caused changes in the values of the characteristic parameters slope and delay (see Results) of <1% and 3%, respectively.

RESULTS

Model of G-activation

Reaction scheme

The model is based on the following scheme:

$$R \xrightarrow{(hv,\ fast)} MI \underset{k_{-1}}{\overset{k_1}{\rightleftharpoons}} MII + G \underset{k_{-2}}{\overset{k_2}{\rightleftharpoons}} MIIG \xrightarrow{k_3,\ GTP} MII + G^*,$$

where R, MI, MII are rhodopsin, metarhodopsin I, metarhodopsin II and G, G* are transducin, activated transducin.

The time course of G* generation is obtained from numerical solution of the corresponding differential equations:

$$d[MII]/dt = k_1[MI] - (k_{-1} + k_2[G])[MII] + (k_3[GTP] + k_{-2})[MIIG] \quad (1)$$

$$d[MIIG]/dt = k_2[G][MII] - (k_3[GTP] + k_{-2})[MIIG] \quad (2)$$

$$d[G^*]/dt = k_3[GTP][MIIG] \quad (3)$$

with $[MI] + [MII] + [MIIG] = \text{const.} = [R^*_0]$ and $[G] + [G^*] + [MIIG] = \text{const.} = [G_0]$.

The concentrations will be understood as two-dimensional, i.e., as the number of G and R molecules per square micrometer.

The function $[G^*](t)$ is characterized by two parameters: maximal slope, i.e., slope in the turning point of the curve, and delay, defined as the time where the tangent in the turning point intersects the baseline. Fig. 2 demonstrates the relationship of these parameters to the time course of $[G^*](t)$, showing an example of $[G^*](t)$ calcu-

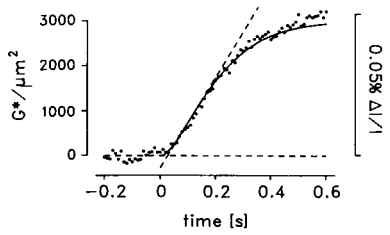

FIGURE 2 ATR-signal and model calculation of G* generation after a flash. The ATR-signal (*points*) was recorded from an intact retina at T = 21.3°C and with flash excitation of rhodopsin R*/R = $2.7 \cdot 10^{-4}$ at time 0. With this flash intensity, the signal amplitude was fully saturated. The solid curve was obtained from numerical solution of Eqs. 1–3 with $[G_0]$ = 3,000/μm², $[R^*_0]$ = 10/μm², [GTP] = 500 μM, α = 1 and the rate constants for 21.3°C (see text). *The peak of the signal is assumed to correspond to the activation of the total G_t pool (3,000/μm²).* The dashed lines demonstrate the characteristic parameters maximal slope, i.e., slope of the tangent in the turning point and delay, i.e., time after the flash where this tangent intersects the baseline. To evaluate the steepest slope of ATR-signals, the tangent in the turning point was drawn by hand.

lated from the reaction model (*solid line*); the data points are a recording of an ATR signal (see below).

Experimental basis

Slope and delay depend on the initial concentrations of the reactants and the time constants of the reaction steps. For the time constants, a whole body of data is available:

Formation of MI (step 0)

This occurs in microseconds and is assumed to be instantaneous.

MI/MII transition (step 1)

Experimental kinetic values for the equilibration at 7°C and pH 7.5 are $1/(k_1 + k_{-1}) \approx 0.3$ s and $1/k_1 \approx 0.8$–1 s (Emeis and Hofmann, 1981; Emeis et al., 1982). We have used $k_1 = 1.1\ s^{-1}$, $k_{-1} = 2.2\ s^{-1}$ for 7°C and an activation energy E_{a1} = 140 kJ/mol (Attwood and Gutfreund, 1980; Hoffmann et al., 1987). From the temperature dependence of measured MII amplitudes, one obtains a value ΔH = 100 kJ/mol. This gives the activation energy for the back-reaction E_{a-1} = 40 kJ/mol which we have used for the model. In the temperature range below 15°C, somewhat higher (10%) activation energies and a lower value for the reaction enthalpy were experimentally obtained (Hoffmann et al., 1987; Parkes and Liebman, 1984). This deviation is neglected.

MII-G complex formation (step 2)

The frequency of collisions between MII and G sets an upper limit for k_2. It depends on the diffusion speed of rhodopsin (~0.5 μm²/s at 20°C [Liebman et al., 1987]) and G_t (unknown). The actual reaction rate may be much lower because, in general, not all collisions lead to a successful coupling of MII and G. (Success of a collision is understood as formation of an MII-G complex with an accessible nucleotide binding site which allows the entry of the activating cofactor GTP.)

The temperature dependence of rhodopsin lateral diffusion has not been determined experimentally for bovine disc membranes. Rhodopsin rotational diffusion data (Coke et al., 1986) are well described by straight Arrhenius curves, indicating the absence of phase transitions in the bovine disc membrane above 5°C, consistent with the result of x-ray diffraction (Chabre, 1975) that, in this range, only a small part of the lipids can take part in rigidification. For mudpuppy porphyropsin, the value for E_a of the lateral diffusion is 48 ± 8 kJ/mol (Drzymala et al., 1984), with a tendency to a lower E_a at higher temperature. The temperature dependence of G_t diffusion is not known; in addition, the collisional success may also depend on temperature. Thus, k_2 is a free parameter of the model that is fitted to our data. For the relative change of k_2 with temperature ($k_{2rel}[T]$) we obtain E_a = 35 kJ/mol, similar to the value for porphyropsin lateral diffusion. This is consistent with the assumption that it depends mainly on the diffusion of R and G_t. This temperature dependence fits to all our data if the absolute value of k_2 is scaled adequately for the two different preparations (see below). Thus, k_2 is given by $\alpha \cdot k_{2rel}(T)$, where k_{2rel} is set to unity at 20°C and α is a temperature-independent scaling factor that accounts for the unknown collisional efficiency between MII and G_t and diffusion speed of G_t. Model calculations were performed for values of α between 0.01 and 1.

To obtain an estimate for k_{-2} we have used the temperature dependence of extra-MII measured in native ROS (pH 7.5) (Emeis, 1982); one obtains a K_D value on the order of 100 G/μm² with no pronounced temperature dependence (see Appendix). Thus, with $K_D = k_{-2}/k_2$ and assuming α = 0.1, one obtains $k_{-2} = 10 \cdot k_{2rel}$ at all temperatures. Here we anticipate that the data from the permeabilized retina (see below), a preparation comparable to the native ROS, are best fit by a value for α ≈ 0.1. For physiological GTP concentration, k_{-2} is almost irrelevant.[2]

Complex dissociation (step 3)

The rate of GTP-induced complex dissociation is k_3 = 0.07 s^{-1} for 2 μM GTP and 1°C and has an apparent

[2]We have also performed the model calculations in Figs. 7 and 8 (500 and 1,000 μM GTP) with $k_{-2} = 0$ at all temperatures; this modification causes a difference in the curves which is within the experimental error and fits the data with the same values for k_2.

activation energy of 165 kJ/mol (measured between −2° and 10°C) (Kohl and Hofmann, 1987). We assume that this temperature dependence extends up to body temperature and that GTP promotes the rate linearly up to cellular (millimolar) concentrations.

Following these considerations, we have generated the rate constants k_1, k_{-1}, k_{2rel}, k_{-2}, and k_3 that provided the data base in all calculations. A set of rate constants for 12 temperatures between 1° and 45° is given in Table 1.

Analytical solution of a simplified model

It is useful to consider a simplified model in which the main determinants of the system become apparent by the simplification $[G](t) = [G_0]$ = constant; in this case the maximal slope is reached when both [MII] and [MIIG] are maximal ($d[MIIG]/dt = 0$ and $d[MII]/dt = 0$). Thus Eqs. 1–3 yield

$$(d[G^*]/dt)_{max} = \frac{[R_0^*] \cdot K_1/(K_1 + 1) \cdot [G_0] \cdot k_2 \cdot [GTP]}{K_1/(K_1 + 1) \cdot [G_0] \cdot k_2/k_3 + k_{-2}/k_3 + [GTP]} \quad (4)$$

with $K_1 = k_1/k_{-1}$.

The model predicts a hyperbolic GTP dependence of the maximal slope of the type $v_{max} \cdot [GTP]/(c_{1/2} + [GTP])$. The hyperbolic character arises from the shift of rate limitation from the dissociation step to the association step when the dissociation rate is promoted by increasing [GTP]. This general character is preserved for $[G](t) = f(t)$ (numerical solutions of equations 1–3), as is seen from the linearized representation in Fig. 3 (*inset*). However, the half saturating GTP concentration $c_{1/2}$ and the maximally obtainable G_t activation rate v_{max} are generally lower than those derived from Eq. 4. Fig. 3 compares $c_{1/2}$ and v_{max} for $[G](t) = f(t)$ and $[G](t) = [G_0]$

TABLE 1 Rate constants used in model calculations of the G_t activation rate (see text)

T	k_1	k_{-1}	k_{2rel}	k_{-2}	k_3
°C	s^{-1}	s^{-1}	$s^{-1}N^{-1*}$	s^{-1}	$s^{-1}\mu M^{-1}$
1	0.295	1.51	0.369	3.69	0.0350
5	0.714	1.94	0.461	4.61	0.0992
7.5	1.22	2.27	0.527	5.27	0.188
10	2.08	2.64	0.602	6.02	0.350
12.5	3.50	3.06	0.686	6.86	0.647
15	5.85	3.55	0.779	7.79	1.18
17.5	9.67	4.09	0.884	8.84	2.14
20	15.9	4.72	1.00	10.0	3.84
25	41.6	6.21	1.27	12.7	12.0
30	106	8.11	1.61	16.1	35.9
35	260	10.5	2.01	20.1	104
45	1450	17.1	3.09	30.9	788

N = number of molecules of R and G_t per square micrometer.

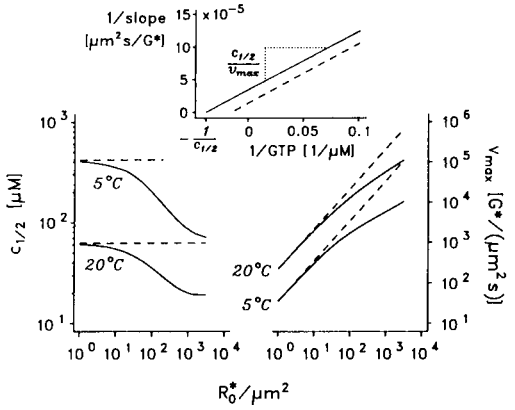

FIGURE 3 Comparison between the maximal G* production rate obtained from numerical solution of Eqs. 1–3 and the approximation given by Eq. 4. Numerical solutions were performed with $[G_0]$ = 3,000/μm² and $\alpha = 0.1$ for several concentrations of GTP and R_0^*; for the rate constants at different temperatures, see text and Table 1. The inset shows the GTP dependence ($[R_0^*]$ = 300/μm², T = 20°C) of the corresponding maximal G* production rates (*slopes*) (values connected by solid line); the dashed line is given by Eq. 4. The representation 1/slope vs. 1/[GTP] linearizes a hyperbolic GTP dependence. Linear regression (correlation coefficient always > 0.99) in this representation yielded the maximally possible G* production rate v_{max} and the half saturating GTP concentration $c_{1/2}$. These values (connected by solid lines) are compared with the approximate $c_{1/2}$ and v_{max} given by Eq. 4 (*dashed lines*) in dependence on $[R_0^*]$ for two different temperatures (5° and 20°C).

in dependence of $[R_0^*]$ at 20° and 5°C ($\alpha = 0.1$). It is seen, that Eq. 4 is a good approximation for small $[R_0^*]$; with 10 R*/μm² the deviation of both $c_{1/2}$ and v_{max} is <20%; at 100 R*/μm² it amounts already to about a factor of two. The deviations arise from the fact that the G-protein has been partly used up when the turning point of $[G^*](t)$ is reached, i.e., $[G_0]$ in Eq. 4 is replaced by $[G](t)$ at the time of the turning point; thus, they increase when the formation of MII is slow (the turning point is reached late) and/or when the decay of G is fast. Factors that contribute to a fast decay of G are high concentrations of MII and high performance of MII-G association and GTP-induced dissociation; although these factors decrease with temperature, the deviations are slightly more prominent at 5°C than at 20°C, due to the pronounced temperature dependence of MII formation that prolongs the time of the turning point.

In the frame of this simplified model, the delay time, as defined above, reflects the time course of the formation of MIIG:

With $[MIIG](t) \sim 1 - \exp(-t/\tau)$

$[G^*](t) \sim \int [MIIG](t)\, dt \sim t - \tau[1 - \exp(-t/\tau)]$.

For $t \to \infty$, $[G^*](t) \sim t - \tau$; extrapolation to $[G^*] = 0$ (intersection with the baseline) yields $td = \tau$.

One simple realization of the exponential case is that the formation of MIIG is rate limited by the formation of MII [$k_1, k_{-1} \ll k_2 \cdot [G_0], (k_3 \cdot [GTP] + k_{-2})$]. In this case:

$$td = \frac{1}{k_1 + K_2/(K_2 + 1) \cdot k_{-1}} \quad (5)$$

with

$$K_2 = \frac{k_3 \cdot [GTP] + k_{-2}}{k_2 \cdot [G_0]}.$$

Eq. 5 represents the upper limit for the delay times in the more realistic solution $[G](t) = f(t)$ and represents a good approximation for small $[R_0^*]$, as seen in Fig. 4, which compares delay times for both solutions (20°C, $\alpha = 0.1$) in dependence on $[R_0^*]$ and for two concentrations of GTP. When the formation of MII is slow compared with the decay of G, e.g., with increasing $[R_0^*]$, the delay shortens quite dramatically. Factors controlling the speed of G activation, like GTP, also influence the extent of the deviation.

Measurements of ATR signals

Fig. 5 compares ATR signals from intact and permeabilized retinae for different temperatures. Both systems have in common a quite dramatic increase of the initial slope with temperature. For example, the signals at the right for 5.9° and 17.1°C differ in their slope by a factor of ~7. The same is observed for the intact retina. In both preparations, the effect of temperature is more pronounced below 15°C. A more quantitative evaluation (see below) reveals that the signals from the permeabilized preparation are generally slower than those from the intact retina and show a different characteristic temperature dependence.

Fig. 2 compares a signal from an intact retina (21.3°C,

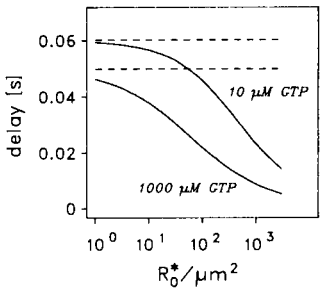

FIGURE 4 Comparison between delay times obtained from numerical solution of Eqs. 1–3 and the approximate delay time given by Eq. 5. Parameters are the same as in Fig. 3; delay times from numerical solutions are given in dependence on $[R_0^*]$ and for two concentrations of GTP (10 and 1,000 µM) with T = 20°C (*solid lines*); dashed lines: Eq. 5.

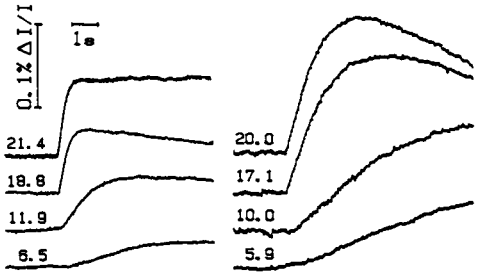

FIGURE 5 ATR-signals from an intact retina (*left*) and an α-toxin permeabilized retina (*right*). Flash excitation R*/R = 2.7 · 10^{-4}; numbers indicate the temperature in °C; the permeabilized retina was supplied with 1 mM GTP.

R*/R = 2.7 · 10^{-4}) to the time course of G_t activation obtained from a model calculation with $[R_0^*] = 10/\mu m^2$, $[G_0] = 3{,}000/\mu m^2$, [GTP] = 500 µM, $\alpha = 1$ and the time constants for 21.3°C as outlined above. The model fits quite well the entire time course of the rising phase of the signal, with realistic assumptions for the initial concentrations of the reactants. To extend the comparison between measured signals and model calculations to the whole temperature range and different $[R_0^*]$, we have analyzed them for the parameters above, maximal slope and delay, that are also demonstrated in Fig. 2. The slope data are normalized to the maximal signal amplitude (A_{max}) of the preparation at room temperature. To determine A_{max}, a sequence of flashes of different intensities was presented to the retina; A_{max} is obtained from a fit of the function $A = A_{max} \cdot [1 - \exp(-a \cdot R^*/R)]$ (not shown, cf. Pepperberg et al., 1988) to the signal amplitudes (A).

A_{max} is a measure of the total concentration of available signal generating reactants which we assume to be identical with the initial concentration of G-proteins ($[G_0]$). Thus the parameter slope/A_{max} represents the normalized G_t activation rate $[G^*]/([G_0] \cdot s)$.

The temperature dependence of A_{max} (Fig. 6) was accounted for by a temperature-dependent change in the entry of $[G_0]$ $[[G_0](T) = [G_{0tot}] \cdot f(T)]$ in the model calculations; $f(T)$ was given by a polynomial fit to the A_{max} values (Fig. 6, *solid line*).[3] Fig. 7 compares slope data of intact (*left*) and permeabilized (*right*) preparations to calculated G-activation rates. For $[G_{0tot}]$ we use $3{,}000/\mu m^2$, assuming that $A_{max}(20°)$ reflects the total

[3]The temperature dependence of A_{max} could, in principle, also arise from a monitor effect (temperature dependence of the scattering properties); in this case, it would be correct to normalize all slopes to the respective $A_{max}(T)$ while the entry of $[G_0]$ in the calculations is temperature independent. We have also tested this possibility and find that the agreement between the data and the calculations is essentially the same.

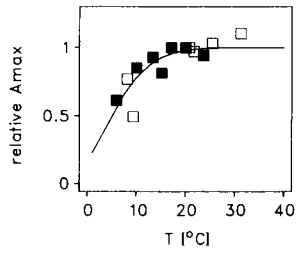

FIGURE 6 Temperature dependence of the maximal amplitude of the ATR-signal (A_{max}). A_{max} was determined from a fit of the function $A = A_{max} \cdot e^{-a \cdot R^*/R}$ (Pepperberg et al., 1988) to the amplitudes (A) of several signals from different flash intensities R*/R; (*open symbols*) Intact retina, (*solid symbols*) permeabilized retina (1 mM GTP); values are normalized to the A_{max} of the respective preparation at 20°C. The solid curve is a polynomial fit to the data.

G-pool. Signals from permeabilized retinae were measured at 1 mM GTP; for intact retina we assumed an internal concentration of 500 μM. In both types of preparation, signals were measured at two different flash intensities ($R^*/R = 2.7 \cdot 10^{-4}$, *solid symbols* and $R^*/R = 1.6 \cdot 10^{-3}$, *open symbols*). With 30,000 rhodopsin molecules per square micrometer this corresponds to $[R_0^*] = 10/\mu m^2$ (*solid lines*) and $35/\mu m^2$ (*dashed lines*). Calculated curves are shown for different values of α.

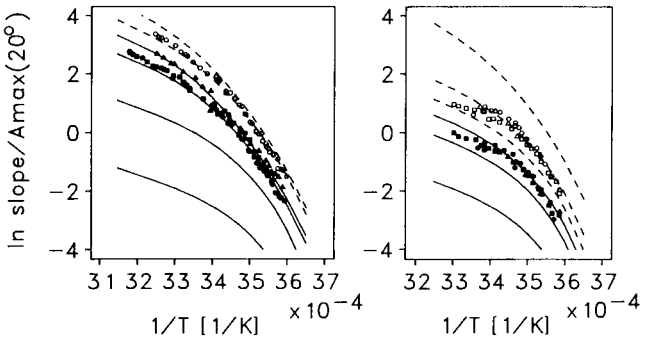

FIGURE 7 Arrhenius plot of the slope of the ATR-signal. The maximal slope of the signals is normalized to the maximal signal amplitude (A_{max}) of the preparation at 20°C and thus has the dimension 1/s; (*open symbols*) flash excitation $R^*/R = 1.16 \cdot 10^{-3}$; (*solid symbols*) $R^*/R = 2.7 \cdot 10^{-4}$. The curves are model calculations of the G_t activation rate, normalized to a total concentration of G-protein $[G_{0tot}] = 3{,}000/\mu m^2$; the initial concentration of activatable G-protein is varied with temperature according to the behavior of the maximal amplitude of the ATR-signal (Fig. 6); initial concentration of photoexcited rhodopsin: $[R_0^*] = 35/\mu m^2$ (*dashed lines*) and $[R_0^*] = 10/\mu m^2$ (*solid lines*); concentration of GTP: 500 μM (*left*) and 1,000 μM (*right*); for further information see text. (*Left panel*) Intact retina; different marker symbols identify different retinae. The set of curves is obtained for α = 1, 0.5 (*dashed lines*) and α = 1, 0.5, 0.1, 0.01 (*solid lines*). (*Right panel*) Permeabilized retina (1 mM GTP); different marker symbols stand for different retinae. The set of curves corresponds to α = 1, 0.1, 0.05 (*dashed lines*) and α = 0.1, 0.05, 0.01 (*solid lines*). The parameter α is a temperature independent scaling factor of the MII-G association rate that accounts for the probability that a collision between the catalytically active rhodopsin and G-protein is successful, and for the unknown diffusion speed of G_t (see text).

The model is able to describe the behaviour of measured slopes quite well, both with respect to the dependence on temperature and the initial concentration of R*, and for both types of preparations. Changing the temperature-independent scaling factor of the MII-G_t association α is sufficient to account for the difference of the preparations, i.e., it adequately transforms the whole Arrhenius plot. Best fit to the data is obtained with α = 0.5–1 for the intact retina and α = 0.05–0.1 for the permeabilized retina.

Analogous to Fig. 7, Fig. 8 shows delay data of permeabilized (*solid symbols*) and intact (*open symbols*) preparations ($R^*/R = 2.7 \cdot 10^{-4}$). No significant difference between the two preparations is observed. Consistently, the model predicts only a small difference between the delay times for α = 0.1 and [GTP] = 1 mM and α = 1 and [GTP] = 0.5 mM (*solid and dashed line*). Furthermore, the measured and the calculated delay times generally agree in their absolute values and their temperature dependence.

The permeabilized preparation also allows the GTP concentration to be varied; we found half saturation of the slope at roughly 100 μM at room temperature (not shown). This is consistent with a $c_{1/2} = 63$ μM which is the prediction of the model for $[G_0] = 3{,}000/\mu m^2$, α = 0.1 and T = 20° (Eq. 4). However, the local GTP concentration might be lowered by GTP consuming dark

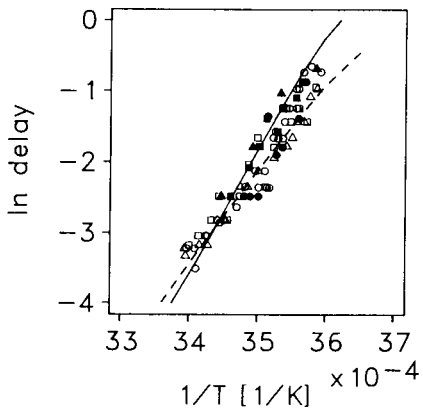

FIGURE 8 Arrhenius plot of the delay times (s) of the ATR-signal. Flash excitation $R^*/R = 2.7 \cdot 10^{-4}$; (*open symbols*) intact retina; (*solid symbols*) permeabilized retina; different marker symbols identify different preparations; data are from part of the signals that constitute Fig. 7, using only recordings with sufficient time resolution for delay evaluation. The curves come from model calculations of G_t activation (see Fig. 7 and text); (*solid line*) [GTP] = 500 μM, α = 1; (*dashed line*) [GTP] = 1,000 μM, α = 0.1.

reactions. To overcome this problem, measurements were routinely performed at saturating GTP concentration (1 mM).

We note that the addition of ATP (up to 500 μM), EGTA (2 mM), or Ca (100 μM) did not enhance the ATR rate of the permeabilized preparation.

DISCUSSION

We have studied the rod visual amplifier in its typical working state in which a few molecules of the light receptor rhodopsin (R) interact sequentially with many molecules of transducin (G_t) to accumulate G_t in its active form. In view of the specific character of R*-G_t interaction (Hamm et al., 1988; König et al., 1989) and its interplay with nucleotide exchange catalysis (Kahlert et al., 1990), we did not consider the possibility that one rhodopsin molecule can quasi-simultaneously activate more than one G_t. Critical for the performance of this system is the time it takes rhodopsin to complete the reaction cycle which results in the release of one molecule of activated G_t. The idea of the study was to use kinetic data in vitro of known partial reaction steps for a reaction model and to compare its prediction with properties of the G_t turnover in situ, as monitored by the ATR light scattering signal.[4] The results presented in this study further support the interpretation of this signal as a linear monitor of G_t activation (Bruckert et al., 1988).[5] We extended the comparison over the measurable range of temperature and tested two different concentrations of activated rhodopsin.

Basis of the reaction model

The kinetic model we have used consists of three steps which contribute to the dynamics of the overall reaction, namely: the equilibration between the active photoproduct metarhodopsin II (MII) and its tautomeric form MI, the association between MII and G_t, and the GTP-induced dissociation. Part of the data we have used to construct the model, namely, those on the MI/MII transition and on the MII-G_t complex dissociation were available from in vitro measurements. With these data and two linear extrapolations (temperature- and GTP-dependence of the dissociation rate), the model is fixed and directly testable in all its parameters, except for the speed and temperature dependence of the MII-G_t association rate (k_2). We have seen that the model is able to fit the data within the measurable temperature range (5–40°) and for both values of [R*]. The fit yields, in turn, values for the parameter k_2; the temperature dependence of k_2 (E_a = 35 kJ/mol) that fits all our data, is consistent with the assumption that it is governed by the temperature dependence of R and G_t diffusion (see Results).

MII-G_t association

Efficiency of collision

By adequately changing the value of a temperature-independent scaling factor (α) of k_2, the difference in speed and temperature dependence of the ATR signals in the intact vs. the permeabilized preparation could be explained. Within the reaction model, there is no other parameter which affords an adequate change of the Arrhenius plot. The interpretation of α in terms of collision success, i.e., the probability of catalytic R-G_t complex formation between the colliding proteins, depends on the assumed diffusion speed of G_t. Direct determinations are lacking.[6] For band 4.1 protein, a peripheral protein of comparable size, the lateral diffusion coefficient in DMPC vesicles is ~6 $\mu m^2/s$ at 35°C (Chang et al., 1981). For the same system and temperature, ~3 $\mu m^2/s$ for rhodopsin is found (Vaz et al., 1982). The lipid/protein ratio in these measurements (800:1 and 3,000:1 vs. 65:1 in the disc membrane) represents a virtually infinite dilution, which explains that the values for D are higher than in the disc membrane (Peters and Cherry, 1982; Saxton and Owicki, 1989). The concentration dependence of diffusion is due to its hindrance by collisions with other particles, an effect to which not only

[4]In the model we have neglected shut off reactions and find that it is sufficient to describe our rising phase data. The preparations used in this study clearly exhibit turn off properties that make the signal recover from the previous flash; (for an analysis of signal recovery in the intact retina at room temperature see Pepperberg et al., 1988). Thus it seems that shut off reactions are at all temperatures too slow to affect the rising phase considerably. Note that the assumption is conservative in the context of our conclusions since an influence of shut off would lead to underestimation of the activation speed.

[5]This implies that the LS change is maximal when all the available G_t is activated. There is, however, no way to determine the size of this activatable G_t-pool from the signal itself; the assumption is intrinsic to all LS studies in situ that the maximal signal reflects activation of the total G_t contained in the rod outer segments (~10% of the total rhodopsin or ~3,000 G_t per μm^2 of the disc membrane). Note that this calibration remains valid no matter whether all or only a constant fraction of the activated G_t physically generates the signal.

[6]An upper limit for G_t diffusion cannot be obtained from the slowing of the electrical signal with increasing viscosity of the cytoplasm (Phillips and Cone, 1985; Phillips and Cone, 1986). G* production and cGMP turnover represent two subsequent amplification stages; the amplifying turnover rates at both stages are multiplicative entries to the risetime of the electrical signal. Slowing of cytoplasmic diffusion is expected to reduce in the first place the cGMP turnover rate, i.e., the gain on the second stage; there is no way to read from the data if and how the first stage is affected.

R* and G_t but also the more abundant R contributes. It will similarly reduce the diffusion speed of integral and peripheral proteins.

G_t might be slower if anchored (Schleicher and Hofmann, 1987; Liebman et al., 1987) by a specific lipid, fatty acid or at rhodopsin itself. Thus diffusion of G_t is, as an upper limit, 2 times faster than of R.

The collision rate between R and G_t can be estimated using the average time interval t_c until a molecule B is captured by an absorber A (Berg and Purcell, 1977). In the two-dimensional case it is given by:

$$t_c = a^2/2 \cdot 1/D_{AB} \cdot [\ln (a/r_{AB}) - 3/4],$$

where a is the average distance of absorbers, r_{AB} is the sum of the effective radii of the reaction partners A and B and D_{AB} is the sum of their diffusion coefficients. For 1 R*/μm^2, $a = (1/\pi)^{1/2}$ μm; the radius of rhodopsin, in cylindrical approximation, is 1.6 nm; for G_t we use the oblate ellipsoid (5:1 axial ratio, MW = 80 kDa) equivalent radius of 5 nm (Liebman et al., 1987); with a rhodopsin diffusion coefficient of D_R = 0.5 $\mu m^2/s$ at 20°C (Liebman et al., 1987), and $D_G = 2 \cdot D_R$, a collision rate of $1/t_c$ = 2.6 s^{-1} per R* and G_t is obtained. With the association rate k_2(20°C) = 0.5–1 s^{-1}, that fits the data from the intact retina, this yields a collisional success of ~30%. This is a lower limit because of upper limit diffusion coefficients and effective radii of R and G_t.

It is interesting to compare to this value the efficiency of rhodopsin transducin collisions in solution. In the three-dimensional case

$$t_c = a^3/3 \cdot 1/D_{AB} \cdot 1/r_{AB}.$$

With $a = (3/4 \cdot 1/\pi)^{1/3}$ μm for 1 R*/μm^3 and D_{AB} = 140 $\mu m^2/s$ (Bruckert, 1989) in solution one obtains ~1,500 collisions per second for each rhodopsin for a G_t concentration of 0.2 μM; by contrast, the measured rate of MII-G_t association for the same [G_t] in biphenyl detergent is <1 s^{-1} (Schleicher et al., 1987). This is in agreement with the typical efficiency of protein–protein interactions in aqueous solution of ~0.1–0.01% (Liebman et al., 1987).

Possible factors responsible for the efficiency

The high efficiency on membranes has certainly to do with the well-organized two-dimensional reaction milieu determined by the membrane surface which gives the possibility of orientation and co-ordination of the binding sites. Surprisingly, the reaction speed was even considerably reduced in the permeabilized preparation which preserves the signal-generating protein inventory for hours of measurement. We do not know the reason for this difference, but a side effect of the α-toxin is unlikely in view of its known mechanism of action (irreversible formation of hexamers in the plasma membrane that do not allow the penetration of the toxin itself, [Füssle et al., 1981]). In addition, association rates derived from G_t activation signals in membrane preparations and from time-resolved measurements of GTP binding in fragmented rods (Liebman and Pugh, 1982) are comparable to those from the permeabilized retina.

A successful association includes the following necessary conditions: (*a*) approach beyond a critical distance by diffusion, (*b*) correct geometrical arrangement of three loops of MII and their respective binding sites at G_t (Hamm et al., 1988; König et al., 1989), and (*c*) loss of GDP from its binding site at G_t and tight three-loop interaction (Kahlert et al., 1990).

Probably most critical for the first two steps is the mode of dark binding of G_t to the membrane surface the nature of which is poorly understood. It is not inconceivable that the mode of dark binding, i.e., the co-ordination and orientation of G_t relative to the membrane, might depend on small soluble factors lost in the permeabilized preparation. Note, however, that there was no difference in the observations for different concentrations of exogenous Ca and ATP, and for Choline vs. Na in the intact system.

The transition from the dark into the light-binding state may be facilitated by the degeneracy of the mutual interaction sites between R and G_t (König et al., 1989). The weak interaction between the "wrong" sites could serve to hold the reaction partners within their mutual critical distance and thereby enhance the efficiency.

MII-G_t complex dissociation

GTP-induced step does not saturate

Linear extrapolation of the complex dissociation rate measured at low [GTP] in vitro (Kohl and Hofmann, 1987) to physiological [GTP] was adequate to fit the data taken in situ in this study; it can be quite generally stated that the high activation speed seen in ATR-like scattering signals of G_t activation (this study; Vuong et al., 1984) would not be approached if the complex dissociation rate would saturate at much lower concentration.

Note, however, that the overall reaction does saturate when the association reaction becomes rate limiting (cf. Eq. 4). When even slower reactions are rate limiting (e.g., in assays limited by GTPase rate or association in solution), the measured reaction rate can even saturate at micromolar GTP.

Mechanism of the dissociation step

Promotion of the GTP-induced step up to millimolar concentrations indicates an apparently very weak affinity

for GTP to the open N-site in the MII-G_t complex. A recent study opens a natural explanation for the low apparent K_D of GTP. It was found that GDP displaces MII from interaction with G_t (Kahlert et al., 1990) and that stable binding of both MII and GDP to G_t exclude each other because binding of the nucleotide is, of necessity, linked with a conformational change in G_t and the breakdown of the MII-G_t complex. Analogous to MII-G_t-GDP, the state MII-G_t-GTP can be interpreted as the unstable transient state adopted in the course of complex dissociation which is reached by the uptake of thermal energy, reflected in the Arrhenius-type activation energy. The link of GTP uptake to the thermally induced transition in the protein explains the high measured value of 165 kJ/mol. It is no longer necessary to assume a pre-equilibrium between a nonexchanging and an exchanging state, separated by a large ΔH (Kohl and Hofmann, 1987).

The unstable GDP- and GTP-binding states of the complex are symmetrically centered around the stable "empty-pocket" state MII-G_t in which the proteins interact via three cytoplasmic loops of R with G_t (König et al., 1989). Note the difference between this transitory MII-G_t state, which is stable in the absence of nucleotide, and the principally unstable transient states MII-G_t-GDP and MII-G_t-GTP.

GDP does not compete effectively

The question arises to which degree the induction by GDP of complex dissociation in the "wrong," nonactivating direction slows the dissociation rate. The G_t activation rate does not appear to be slowed by the (unknown but not negligible) amount of GDP which is present in our preparations. This is consistent with measurements of dissociation signals on G_t-recombined membranes, which show that GDP slows the rate rather inefficiently (half suppression at 100 μM GDP with [GTP] = 20 μM [Kahlert et al., 1990]). In any case, an influence of GDP would lead to an underestimation of the G_t activation rate and would therefore not change our conclusions.

Amplification needs high [GTP]

In this context, it is interesting to note that the visual cascade really needs 0.5–1 mM GTP to perform with the speed seen in the ATR signals. In view of the high turnover of G_t, which is comparable to the estimated nucleotide concentrations, [GTP] will fall and [GDP] will rise dramatically during a flash-induced turnover of the G_t pool. High absolute concentrations, the relative inefficiency of GDP vs. GTP discussed above, and a rapid turnover of the nucleotides (Dawis et al., 1988) are equally important for the performance of the G_t amplifying step.

Speed of G-protein activation

Independent of the model calculations, from the LS data (Fig. 7) and the assumption that 3,000 $G_t/\mu m^2$ (i.e., the whole G_t pool) are activated when the amplitude of the signal is maximal, turnover numbers of G_t can be determined (ordinate value in Fig. 7 times 3,000, divided by the number of R* per μm^2). One obtains 30, 120, 800, 2,500, and 4,000 G_t per R* and second at 5, 10, 20, 30, 37°C respectively.

APPENDIX

Determination of the dissociation constant $K_D = k_{-2}/k_2$ between G_t and MII from extra-MII data

In a ROS-preparation at pH 7.5 at 10°C $([MII]/[MII_{max}])_1 \approx 0.9$ is measured for the first flash; for later flashes (when no extra MII is formed, because all the G_t is already bound) $([MII]/[MII_{max}])_\infty \approx 0.4$ is obtained (Emeis, 1982).

$[MII_{max}]$ is equivalent to the total concentration of photoexcited rhodopsin $[R_0^*]$.

With

$$K_1 = [MII]/]MI], \quad (1)$$

$$K_2 = [MIIG]/([MII][G]), \quad (2)$$

$$[R_0^*] = [MI] + [MII] + [MIIG], \text{ and} \quad (3)$$

$$[G_0] = [G] + [MIIG] \text{ one obtains} \quad (4)$$

$[MIIG]^2 - [MIIG]([R_0^*] + [G_0] + 1/K_2(1 + 1/K_1)) + [R_0^*][G_0] = 0$ or

$$1/K_2 = K_D = \frac{[MIIG]^2 - [MIIG]([R_0^*] + [G_0]) + [R_0^*][G_0]}{(1 + 1/K_1)[MIIG]} \quad (5)$$

K_1 can be determined from the MII level evoked by later flashes ($[G_0] = 0$): $([MII]/[MII_{max}])_\infty = [MII]/([MII] + [MI])$; with (1) this yields

$$K_1 = \frac{([MII]/[MII_{max}])_\infty}{1 - ([MII]/[MII_{max}])_\infty} \approx 0.7. \quad (7)$$

[MIIG] is determined from the first flash: $([MII]/[MII_{max}])_1 = ([MII] + [MIIG])/[R_0^*]$; (1) and (3) yield $[MII] = ([R_0^*] - [MIIG])K_1/(K_1 + 1)$; using this, one obtains

$$[MIIG] = (([MII]/[MII_{max}])_1(K_1 + 1) - K_1)[R_0^*]$$
$$\approx 0.8[R_0^*]. \quad (8)$$

The flash activation of rhodopsin was ~2%; with 30,000 rhodopsin molecules/μm^2. This means $[R_0^*] \approx 600/\mu m^2$; we assume $[G_0] \approx 1{,}500/\mu m^2$. Using these concentrations and the value for $K_1 = 0.7$, Eq. 5 yields $K_D \approx 100/\mu m^2$.

Similar values are obtained from data at other temperatures; for example $K_D \approx 100/\mu m^2$ at 5°C and $K_D \approx 90/\mu m^2$ at 0°C.

We acknowledge the technical assistance of I. Bäumle. The α-toxin was a generous gift from Behring-Werke, Marburg, FRG.

This work was supported by the Deutsch Forschungsge meinschaft (SFB 60 and SFB 325).

Received for publication 5 June 1990 and in final form 10 September 1990.

REFERENCES

Attwood, P. V., and H. Gutfreund. 1980. The application of pressure relaxation to the study of the equilibrium between metarhodopsin I and II from bovine retinas. *FEBS (Fed. Eur. Biochem. Soc.) Lett.* 119:323–326.

Baylor, D. A., T. D. Lamb, and K.-W. Yau. 1979. Responses of retinal rods to single photons. *J. Physiol.* 288:613–634.

Berg, H. C., and E. M. Purcell. 1977. Physics of chemoreception. *Biophys. J.* 20:193–219.

Bruckert, F. 1989. Etude in situ, par diffusion de lumiere infrarouge, de la transducine dans les batonnets retiniens: attachement aux membranes des disques et cinetique d'activation par la rhodopsine photoexcitee. Ph.D. thesis. Universite Joseph Fourier, Grenoble, France. 8–9.

Bruckert, F., T. M. Vuong, and M. Chabre. 1988. Light and GTP dependence of transducin solubility in retinal rods. *Eur. Biophys. J.* 16:207–218.

Caretta, A., and P. J. Stein. 1985. cGMP- and phosphodiesterase-dependent light-scattering changes in rod disk membrane vesicles: Relationship to disk vesicle-disk vesicle aggregation. *Biochemistry.* 24:5685–5692.

Chabre, M. 1975. X-Ray diffraction studies of retinal rods I. Structure of the disc membrane, effect of illumination. *Biochim. Biophys. Acta.* 382:322–335.

Chabre, M., and P. Deterre. 1989. Molecular mechanism of visual transduction. *Eur. J. Biochem.* 179:255–266.

Chang, C.-H., H. Takeuchi, T. Ito, K. Machida, and S. Ohnishi. 1981. Lateral mobility of erythrocyte membrane proteins studied by the fluorescence photobleaching recovery technique. *J. Biochem.* 90:997–1004.

Coke, M., C. J. Restall, C. M. Kemp, and D. Chapman. 1986. Rotational diffusion of rhodopsin in the visual receptor membrane: effects of temperature and bleaching. *Biochemistry.* 25:513–518.

Cone, R. A. 1972. Rotational diffusion of rhodopsin in the visual receptor membrane. *Nature New Biol.* 236:39–43.

Dawis, S. M., R. M. Graeff, R. A. Heyman, T. F. Walseth, and N. D. Goldberg. 1988. Regulation of cyclic GMP metabolism in toad photoreceptors. *J. Biol. Chem.* 263:8771–8785.

Drzymala, R. E., H. L. Weiner, and P. A. Liebman. 1984. A barrier to lateral diffusion of porphyropsin in necturus rod outer segment disks. *Biophys. J.* 45:683–692.

Emeis, D. 1982. Zur Ankopplung enzymatischer Reaktionen an die Rhodopsin-Photolyse: simultane zeitaufgelöste Messungen von Lichtstreuung-und Absorptionsänderungen. Ph.D. thesis. Albert-Ludwigs-Universität, Freiburg, FRG.

Emeis, D., and K. P. Hofmann. 1981. Shift in the relation between flash-induced metarhodopsin I and metarhodopsin II within the first 10% rhodopsin bleaching in bovine disc membranes. *FEBS (Fed. Eur. Biochem. Soc.) Lett.* 136:201–207.

Emeis, D., H. Kühn, J. Reichert, and K. P. Hofmann. 1982. Complex formation between metarhodopsin II and GTP-binding protein in bovine photoreceptor membranes leads to a shift of the photoproduct equilibrium. *FEBS (Fed. Eur. Biochem. Soc.) Lett.* 143:29–34.

Füssle, R., S. Bhakdi, A. Sziegoleit, J. Tranum-Jensen, T. Kranz, and H. J. Wellensiek. 1981. On the mechanism of membrane damage by staphylococcus aureus α-toxin. *J. Cell Biol.* 91:83–94.

Gilman, A. G. 1987. G-proteins: transducers of receptor generated signals. *Annu. Rev. Biochem.* 56:615–649.

Hamm, H. E., D. Deretic, A. Arendt, P. A. Hargrave, B. König, and K. P. Hofmann. 1988. Site of G Protein binding to rhodopsin mapped with synthetic peptides from the α subunit. *Science (Wash. DC).* 241:832–835.

Hoffmann, W., F. Siebert, K. P. Hofmann, and W. Kreutz. 1987. Two distinct rhodopsin molecules within the disc membrane of vertebrate rod outer segments. *Biochim. Biophys. Acta* 503:450–461.

Hofmann, K. P. 1986. Photoproducts of rhodopsin in the disc membrane. *Photobiochem. Photobiophys.* 13:309–338.

Hofmann, K. P., R. Uhl, W. Hoffmann, and W. Kreutz. 1976. Measurements of fast light-induced light-scattering and absorption changes in outer segments of vertebrate light sensitive rod cells. *Biophys. Struct. Mech.* 2:61–77.

Kahlert, M. 1986. Simultane Messungen und Modellrechnungen von Lichtstreusignalen und Elektroretinogrammen der Rinderretina. Masters thesis. Albert-Ludwigs Universität, Freiburg, FRG.

Kahlert, M., and K. P. Hofmann. 1988. In situ investigation of the amplification mechanism in retinal rods. *In* Spectroscopy of Biological Molecules—New Advances. E. D. Schmid, F. W. Schneider, and F. Siebert, editors. John Wiley and Sons. 483–486.

Kahlert, M., B. König, and K. P. Hofmann. 1990. Displacement of rhodopsin by GDP from three loop interaction with transducin depends critically on the diphosphate β-position. *J. Biol. Chem.* 265:18928–18932.

Kamps, K. M. P., J. Reichert, and K. P. Hofmann. 1985. Light-induced activation of the rod phosphodiesterase leads to a rapid transient increase of near infrared light scattering. *FEBS (Fed. Eur. Biochem. Soc.) Lett.* 188:15–20.

Kohl, B., and K. P. Hofmann. 1987. Temperature dependence of G-protein activation in photoreceptor membranes—Transient extra metarhodopsin II on bovine disc membranes. *Biophys. J.* 52:271–277.

König, B., A. Arendt, J. H. Mc Dowell, M. Kahlert, P. A. Hargrave, and K. P. Hofmann. 1989. Three cytoplasmic loops of rhodopsin interact with transducin. *Proc. Natl. Acad. Sci. USA.* 86:6878–6882.

Kühn, H., N. Bennett, M. Michel-Villaz, and M. Chabre. 1981. Interactions between photoexcited rhodopsin and GTP-binding protein: Kinetic and stoichiometric analysis from light scattering changes. *Proc. Natl. Acad. Sci. USA.* 78:6873–6877.

Lamb, T. D. 1987. Sources of noise in photoreceptor transduction. *J. Opt. Soc. Am. A.* 4:2295–2300.

Lewis, J. W., J. L. Miller, J. Mendel-Hartvig, L. I. Schaechter, D. S. Kliger, and E. A. Dratz. 1984. Sensitive light scattering probe of enzymatic processes in retinal rod photoreceptor membranes. *Proc. Natl. Acad. Sci. USA.* 81:743–747.

Liebman, P. A., and G. Entine. 1974. Lateral diffusion of visual pigment in photoreceptor disc membranes. *Science (Wash. DC).* 185:457–459.

Liebman, P. A., and Pugh, E. N., Jr. 1982. Gain, speed and sensitivity of GTP binding vs PDE activation in visual excitation. *Vision Res.* 22:1474–1480.

Liebman, P. A., K. R. Parker, and E. A. Dratz. 1987. The molecular mechanism of visual excitation and its relation to the structure and composition of the rod outer segment. *Annu. Rev. Physiol.* 49:765–791.

Parkes, J. H., and P. A. Liebman. 1984. Temperature and pH dependence of the metarhodopsin I-metarhodopsin II kinetics and equilibria in bovine rod disc membrane suspensions. *Biochemistry.* 23:5054–5061.

Pepperberg, D. R., M. Kahlert, A. Krause, and K. P. Hofmann. 1988. Photic modulation of a highly sensitive, near-infrared light-scattering signal recorded from intact retinal photoreceptors. *Proc. Natl. Acad. Sci. USA.* 85:5531–5535.

Peters, R., and R. J. Cherry. 1982. Lateral and rotational diffusion of bacteriorhodopsin in lipid bilayers: experimental test of the Saffman-Delbrück equations. *Proc. Natl. Acad. Sci. USA.* 79:4317–4321.

Phillips, E., and R. A. Cone. 1985. Cytoplasmic diffusion rates in rod outer segments: how much do the discs slow diffusion along the rod? *Invest. Ophthal. Mol. & Visual Sci.* 26(Suppl.):168.

Phillips, E., and R. A. Cone. 1986. Do diffusion rates in the cytoplasm or the membrane limit the response speed of the vertebrate rod? *Biophys. J.* 49:277*a*. (Abstr.)

Poo, M., and R. A. Cone. 1974. Lateral diffusion of rhodopsin in the photoreceptormembrane. *Nature (Lond.).* 247:438–442.

Saxton, M. J., and J. C. Owicki. 1989. Concentration effects on reactions in membranes: rhodopsin and transducin. *Biochimica Biophys. Acta.* 979:27–34.

Schleicher, A., and K. P. Hofmann. 1987. Kinetic study on the equilibrium between membrane-bound and free photoreceptor G-protein. *J. Membr. Biol.* 95:269–279.

Schleicher, A., R. Franke, K. P. Hofmann, H. Finkelmann, and W. Welte. 1987. Deoxylysolecithin and a new biphenyl detergent as solubilizing agents for bovine rhodopsin—functional test by formation of metarhodopsin II and binding of G-protein. *Biochemistry.* 26:5908–5916.

Stryer, L. 1986. Cyclic GMP cascade of vision. *Annu. Rev. Neurosci.* 9:87–119.

Vaz, W. L. C., M. Criado, V. M. C. Madeira, G. Schoellmann, and T. M. Jovin. 1982. Size dependence of the translational diffusion of large integral membrane proteins in liquid-crystalline phase lipid bilayers. A study using fluorescence recovery after photobleaching. *Biochemistry.* 21:5608–5612.

Vuong, T. M., M. Chabre, and L. Stryer. 1984. Millisecond activation of transducin in the cyclic nucleotide cascade of vision. *Nature (Lond.).* 311:659–661.

Wagner, R., N. J. P. Ryba, and R. Uhl. 1987. The amplified P-signal, an extremely photosensitive light scattering signal from rod outer segments, which is not affected by pre-activation of phosphodiesterase with Gα-GTP-τ-S. *FEBS (Fed. Eur. Biochem. Soc.) Lett.* 221:253–259.